ORIGINAL PAPER

Estimation of ground vibration and settlement during underground tunneling in Kolkata, India

Aniruddha Sengupta [1] · Raj Banerjee [2,3] · Srijit Bandyopadhyay [2,3]

Abstract

A second underground metro line consisting of two parallel tunnels of diameter 6.1 m and 15 m apart is under construction through the busiest commercial areas of Kolkata, India. The crest of the tunnels is located at an average depth of 17.6 m below the ground. The Kolkata subsoil consists of mainly soft silty clays. Three old heritage buildings on raft foundations are located within the near proximity of the metro tunnels. This paper quantifies the possibility of damages to these old heritage buildings due to settlement and/or vibration during the subsurface tunnel construction based on a static and dynamic finite element analysis to satisfy the administration and the people of Kolkata regarding the safety of the surrounding structures during the tunneling and to obtain the required permissions for the work. The results of the static finite element analyses are compared with some well accepted empirical methods to quantify ground settlements due to tunneling of the E-W metro. The numerical results are also compared with the field instrumentation data recently made available. The numerical analyses and the two empirical methods show reasonable match for the settlements near the centerlines of the tunnels. But the empirical methods start to under-predict settlements with distance. Around 20 m from the centerline of 2nd tunnel, the numerical predictions match reasonably well with the measured values of the settlements. However, at 30 m distance, the numerical analyses somewhat under-predict the settlements. Even though it may have some limitations, a proper finite element analysis is strongly recommended over other empirical methods to estimate deformations due to underground tunneling. The settlements and the angular distortions in the three heritage buildings are found to be within tolerable limits. The peak particle velocity at the ground surface, obtained from the dynamic finite element analyses, is found to be about 0.003 mm/s due to the vibration during tunnel construction. This value is significantly less than the allowable value of 1 mm/s. No adverse effect due to the twin tunnel construction has been reported so far.

✉ Aniruddha Sengupta
sengupta@civil.iitkgp.ac.in

Raj Banerjee
rajbanerji90@gmail.com

Srijit Bandyopadhyay
srijit15@gmail.com

[1] Indian Institute of Technology, Kharagpur 721302, India

[2] IIT Kharagpur, kharagpur, India

[3] BARC, Mumbai, India

Introduction

Kolkata is a highly populated cosmopolitan city located in the eastern part of Indian. It used to be the capital of India during the British era, and for this reason, the city has a large number of old building which are considered to be heritage monuments. The city has two major train stations on either side of the River Ganges which is flowing along the western side of the city. The existing underground metro rail is running along the length of Kolkata (parallel to the River Ganges). A second underground metro railway, known as E-W metro, is at present under construction across the width of the city connecting the main business hub (Brabourne Road) of Kolkata to the two main railway stations (Howrah Station and Sealdah Station). This metro line will also eventually connect the train

Fig. 1 Route of E-W Metro in Kolkata
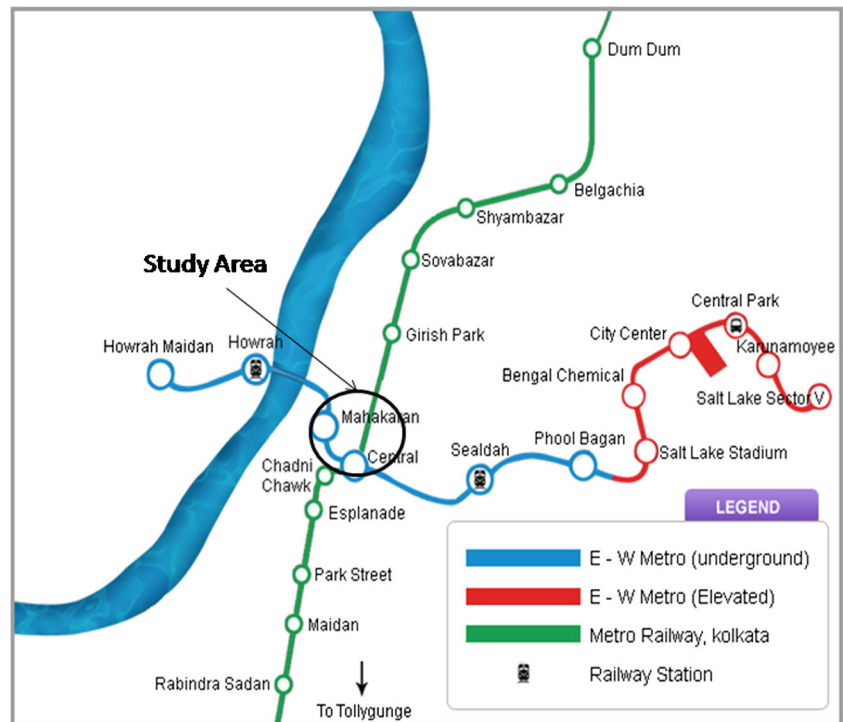
stations and the city to the existing international airport of the area. Figure 1 shows the locations of the new metro line under construction and the present study area (Brabourne Road).

Two 6.1 m in diameter circular tunnels, 15 m apart from center to center, are under construction through the very congested business areas (Brabourne Road) of Kolkata. The crowns of the tunnels are located at a depth of 17.6 m below the ground level (KMRC 2015a, b, c). Figure 2 shows an aerial view of Brabourne Road within Kolkata and the location of the present study area.

A number of old heritage structures, constructed during the British period in India, are located within the near proximity of the E-W metro line. Three of these old

Fig. 2 A view of the study area (Brabourne Road, Kolkata) along the Route of E-W Metro

buildings are within the present study area, along the Brabourne Road. These heritage structures are on either sides of the road and between 19 and 30 m from the tunnels' centerline. These old heritage structures are 2- to 3-storey high masonry buildings resting on raft foundation. The raft foundations extend up to a depth of 2 m below the ground. The structural damage to these old structures due to excessive deformations and/or vibration during the tunnel constructions is a concern. The adjacent relatively new reinforced concrete buildings are on pile foundations and considered to be less vulnerable to the ground vibration and settlement due to the underground excavation of the tunnels.

Before the beginning of the E-W tunnel construction within the city of Kolkata, a number of litigation were filed by the owners of the old heritage buildings raising a concern regarding the safety of these buildings during the subsurface tunneling. Upon request from the owner of the E-W metro (KMRC), numerical and analytical analyses of the tunnel construction were performed to satisfy the queries from the owners of the buildings and the citizens of Kolkata regarding the possibility of damages to the old heritage buildings due to settlement and/or vibration during the underground tunnel construction and also to obtain the required administrative approvals for the tunneling work through the city. The present paper delineates these static and dynamic analyses performed to evaluate the possible settlement and vibrations of the buildings during the E-W tunnel construction.

The construction of subsurface tunnels using Earth Pressure Balance-Tunnel Boring Machine (EPB-TBM) for underground roadways and railways is becoming increasingly common in the metro cities worldwide due to shortage of space on the surface. However, several literatures (Camos et al. 2014; Zhang et al. 2013) have reported damages to the structures on the ground surface due to such construction of underground tunnels especially in soft ground. Predicting how a subsurface tunnel construction can affect the ground surface and the structures on it is one of the major concerns. Unfortunately, the current soil settlement predictions are still largely based on empirical relationships (Peck 1969; Mair et al. 1996; FHWA 2009) put forward based on the experience gained from past projects and they are often lacking in adequate case-specificity (Mair and Taylor 1997). The expected level of risk is defined by the concept of "volume loss" of the subsurface materials as obtained from previous tunneling experiences under similar circumstances. The rate of volume loss is correlated to the expected settlement of the surrounding soil via empirical (Peck 1969), analytical (Verruijt 1997), or numerical (Komiya et al. 1999; Sugimoto and Sramoon 2002; Sugimoto et al. 2007; Nagel et al. 2010, Festa et al. 2013) analyses. Another important concern in subsurface tunneling is the ground vibration generated by a TBM machine. Very limited relevant literature (Mooney et al. 2014) is available on this subject. Mooney et al. (2014) have shown that the vibration transmitted through a ground due to EPB-TBM interacting with the ground during a tunneling operation in Seattle, Washington (USA), depends on the surrounding geologic formation.

During the course of this study, a static analysis of the construction sequences of the twin tunnels has been performed using a computer software called PLAXIS2D (Plaxisbv 2012) to study the ground settlements at the locations of the heritage buildings. In the absence of any available field data during this study period, these numerical results are compared with the corresponding values obtained from the well established empirical methods proposed by Mair et al. (1996) and FHWA (2009). As per recommendations during this study, the three heritage buildings located in the vicinity of tunnel alignment are instrumented to obtain real time values of deformations during the tunnel construction. As part of these instrumentation data is available at this time, a comparison between them and the numerical results is also shown. A dynamic analysis of the tunnels is additionally performed where the construction related vibrations within the tunnels are modeled by a synthetic white noise, to roughly estimate the ground vibrations at the heritage building locations. The results obtained from the present analyses are utilized for the structural analyses of the heritage buildings to check their stability. However, the structural stability analyses of these buildings are not within the scope of the present paper and are not presented.

## Kolkata subsoil and their engineering properties

The subsoil profile of Kolkata along the routes of new metro line is determined from the data obtained from several boreholes driven in the area. Undisturbed soil samples are recovered from different depths and tested in the laboratory for their classification, density, water content, permeability, undrained, and drained shear strengths. The subsoil of Kolkata is essentially soft clayey (silty clay to clayey silt) soil deposited over time by Ganges. At a greater depth, layers of dense sand are located. Figure 3 depicts the typical soil profile with depth in Kolkata near Brabourne Road. The corresponding soil properties are also shown. As per the borehole data, the first 2 m of Kolkata soil is a fill material with a hydraulic conductivity of 5 × 10^{-5} m/s. The ground water table, as measured at the boreholes, is located at 1 m below the surface. From 2 to 15.4 m, the soil is clayey silt to silty clay (designated as unit 2). Between 15.4 and 19.5 m, the soil is medium silty clay (designated as unit 3a). Below a depth of 19.5 m, the soil is silty clay (with unit 3b designation) with some sand. The present soil profile of Kolkata at the project location is found to be matching quite well with that given by Bandyopadhyay et al. (2019) for Kolkata based on a large number of boreholes and test data. The shear strengths of the soil units are given in Table 1.

In the absence of any consolidation test data (which are not done during the course of this study, as they take some time and could delay the start of the work), the in situ clayey soils are considered to be normally consolidated, to be on the conservative side, with an over consolidation ratio (OCR) of 1. The average undrained strength (C_u) of these clayey soils are found to be 31, 70, and 55 kPa, respectively, from the limited number of laboratory undrained test results available. The shear strengths (c' = effective cohesion, ϕ' = effective friction angle, and γ = unit weight) of the top 2 m of backfill soil are considered to be same as those for the silty clay/clayey silt (unit 2). However, their values of the hydraulic conductivity are different. The average index of plasticity (PI) for the soil types 2, 3b, and 3b (refer to Fig. 3) are 30, 45, and 35, respectively. The at-rest earth pressure coefficient for all the soil units is considered to be 0.5. The Poisson's ratio (ν_s) of the soils is taken as 0.3. The values of the elastic modulus presented in Table 1 are the average tangent modulus for the soils obtained from the laboratory triaxial tests on the representative soil samples. For the top 15 m of soft silty clay, the deformation modulus (E_s) of this soil is 18,600 kPa from the laboratory triaxial tests done on the undisturbed samples. The value of the E_s is found to be within the limits for the modulus of a soft clayey soil reported in the literature (Kulhawy and Mayne 1990) and also correlating well with the values of C_u and PI

Table 1   Soil properties

Soil type	Permeability, k (m/s)	Unit wt., γ (kN/m^3)	Undrained strength, C_u (kPa)	Cohesion, c' (kPa)	Friction angle, ϕ' (deg.)	Deformation modulus, E_s (kPa)
Fill	5×10^{-5}	--	--	--	--	--
Silty clay (unit 2)	10^{-7}	18.5	31.0	1.0	25	18,600
Medium silty clay (unit 3a)	10^{-9}	18.5	70.0	0.0	31	31,500
Silty clay (unit 3b)	10^{-6}	18.5	55.0	0.0	29	27,500

(USACE 1990). The silty clay between 15 and 20 m is a medium clay with E_s of 31,500 kPa. This value is also found to be within the range for a medium clay reported in the literature and correlating well with the respective values of C_u and PI. For the silty clay layer below 20 m, the value of E_s of 27,500 kPa is obtained from the laboratory triaxial tests. This value is also found to be within the range for a medium clay reported in the literature and found to be correlating well with the corresponding values of C_u and PI for this layer.
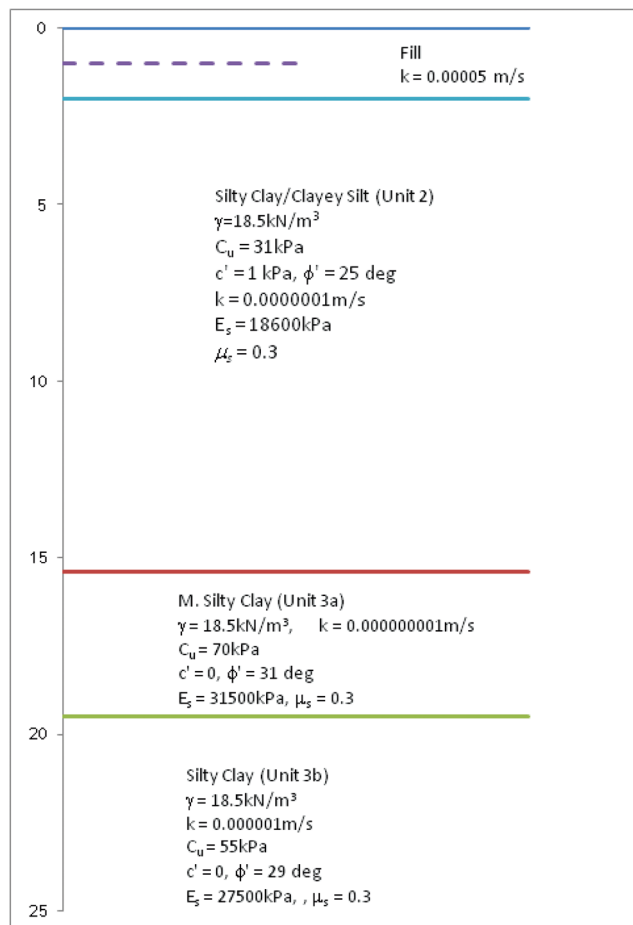
Fig. 3 Subsoil profile and their properties at the study area (Brabourne Road, Kolkata)

Numerical analyses

The finite element analyses are performed using a commercial software called PLAXIS2D (Plaxisbv 2012). The program is suitable for solving 2D, plane strain, coupled, soil-structure interaction problems where large strains are envisaged. The basic equation solved at elemental level is given by

$$\dot{\sigma} = D\left(\dot{\varepsilon_e}\right) = D\left(\dot{\varepsilon} - \dot{\varepsilon_p}\right) \qquad (1)$$

where σ represents stresses and ε_e and ε_p are the elastic and plastic strains, respectively, at a point within an element. D is a stiffness matrix at elemental level, and the superscript (˙) indicates the rate or incremental form of the quantity.

The subsoil domain is numerically discretized by 8-node rectangular and 6-node triangular iso-parametric elements. The constitutive behaviors of the subsoil are modeled by nonlinear, elasto-plastic, Mohr-Coulomb model. Though a number of advanced soil models are available, they are not utilized in this study due to the lack of test data on the consolidation and the unloading-reloading behaviors of the soils. In the Mohr-Coulomb model, the unit weight, γ; the effective cohesion, c'; the effective friction angle, ϕ'; angle of dilatancy, ψ'; and elastic modulus, E_s, are specified for the soils. The angle of dilatancy, ψ', is assumed to be zero for all the soils. Besides these parameters, the permeability, k, for the soils is also specified. Table 1 shows the values of the above parameters for all the soil units considered here.

The tunnels are 6.1 m in diameter, and they are 15 m apart (centerline to centerline). The tunnels have concrete lining (M40 grade concrete) of 350 mm thickness. The tunnel linings are modeled by beam element. The concrete linings of the tunnels are assumed to be elastic and impervious. The deformation modulus and the Poisson's ratio of the concrete linings of the tunnels are $E_{conc} = 3.162E+07$ kPa and $\upsilon_{conc} = 0.15$, respectively.

To maintain compatibility between the soil elements and the concrete lining elements (soil elements have 2 degrees of freedom while the beam elements have 3 degrees of freedom), interface elements are placed between them. An interface element has 2 degrees of freedom at each node. The interface has

an imaginary (virtual) thickness to which the material parameters are assigned. The virtual thickness is determined by the virtual thickness factor times the average element size. The element size mainly depends on the global coarseness of the finite element mesh. The virtual thickness factor used in this study is 0.1, which is a default value. When the interface is in elastic stage, the stress and strain increments are related to the interface normal stress, σ_n, and shear stress, τ_n, as follows:

$$\begin{bmatrix} \dot{\tau}_n \\ \dot{\sigma}_n \end{bmatrix} = \begin{bmatrix} k_s & 0 \\ 0 & k_n \end{bmatrix} \begin{bmatrix} \dot{\varepsilon}_s^e \\ \dot{\varepsilon}_n^e \end{bmatrix} \tag{2}$$

When the interface is in plastic state, the incremental stresses and strains at the interface are related as follows:

$$\begin{bmatrix} \dot{\tau}_n \\ \dot{\sigma}_n \end{bmatrix} = \left[\begin{pmatrix} k_s & 0 \\ 0 & k_n \end{pmatrix} - \frac{1}{(k_s - k_n \tan(\phi)\tan(\psi))} \begin{pmatrix} k_s^2 & -k_s k_n \tan(\phi) \\ -k_s k_n \tan(\psi) & k_s^2 \tan(\phi)\tan(\psi) \end{pmatrix} \right] \begin{bmatrix} \dot{\varepsilon}_s^e \\ \dot{\varepsilon}_n^e \end{bmatrix} \tag{3}$$

An interface reduction factor (R) of 0.67 is used for the reduction of the cohesion and the angle of internal friction at the interface. The interface normal and shear subgrade reactions (K_n and K_s in Pa/m) PLAXIS2D (Plaxisbv 2012) are given by

$$K_n = K_s = 10 \max \left[\frac{\left(K + \frac{4}{3}G \right)}{\Delta z_{\min}} \right] \tag{4}$$

where K is the bulk modulus of the soil, G is the shear modulus of the soil, and $\Delta z_{\min}$ is the smallest width (0.025 m) of the adjoining zone in the normal direction to the interface.

In the numerical analyses, the two vertical boundaries on the sides are located 50 m from the tunnels. These boundaries are assumed to be on roller, and only vertical movements are allowed. The bottom horizontal boundary is 20 m below the tunnels, and only horizontal movements are allowed. The crown and invert of both the tunnels at Brabourne Road are located at a depth of 17.6 m and 23.7 m, respectively. The numerical discretization of the subsoil layers and the tunnels is shown in Fig. 4.

As per KMRC (2015a, b, c) report, both the tunnels are being excavated by earth pressure balance shield (EPBS) method, but not at the same instance at a location. At any section, the second tunnel is constructed after the first tunnel has advanced by a horizontal distance of at least 120 m. The ground loss due to seepage of ground water during the tunnel constructions and the grout loss during the tunnel construction are not considered directly. The ground loss due to tunneling is indirectly by assuming a value for the volume loss (V_L) in the analyses. The volume loss (V_L) is defined as the volume of loss material per length in the region of the tunnel (difference between the total volume of the excavated tunnel and the recovered volume of the excavated material from the subsurface) during the tunneling, divided by the total volume of the excavated tunnel per length. It is usually expressed in terms of

percentage. Two extreme cases of volume loss (V_L) due to tunneling are considered. In the first case, a 2% V_L, as suggested by FHWA (2009), is considered. This represents a poor tunneling practice with a closed face TBM within a raveling ground. A V_L of 0.25% is considered in the next case. This situation represents a good tunneling practice with a tight control of face pressure within the closed face TBM in a slowly raveling or squeezing soil. As per Gouw (2005), this value of V_L shows good match with the observed settlements during the tunneling by EPBS method in soft marine clay of Singapore. To simulate the loss in volume of soil due to tunneling action, the contraction method is used in PLAXIS 2D. In this method, a certain percentage (0.25 and 2% in this study) of the original cross sectional area of the tunnels is reduced during the stage construction of the tunnels.

In the numerical analyses, the heritage buildings located within the area are not modeled. The effects of the weights and stiffness of these buildings are not accounted for in these analyses. The differential settlements at the foundation of these buildings are estimated from the numerical analyses and detailed structural analyses of these buildings are performed. These structural analyses are not presented in this paper. At the beginning of the finite element analyses, the equilibrium of the whole soil subsurface domain without the two tunnels is maintained. Next, the tunnels are constructed one after another. The deformations and stresses are computed at the end of the construction of each tunnel.

Settlements due to tunnel constructions

The alignment of the proposed tunnels at the E-W metro project in Kolkata is such that the Currency Building, the exchequer of British-India and a heritage structure, is located 30 m from the second (right) tunnel. Another two heritage buildings, Meghen David and Bethel Synagogues, are located 20 m and 19 m from the centerline of the right side (2nd) tunnel (KMRC 2015a, b, c).

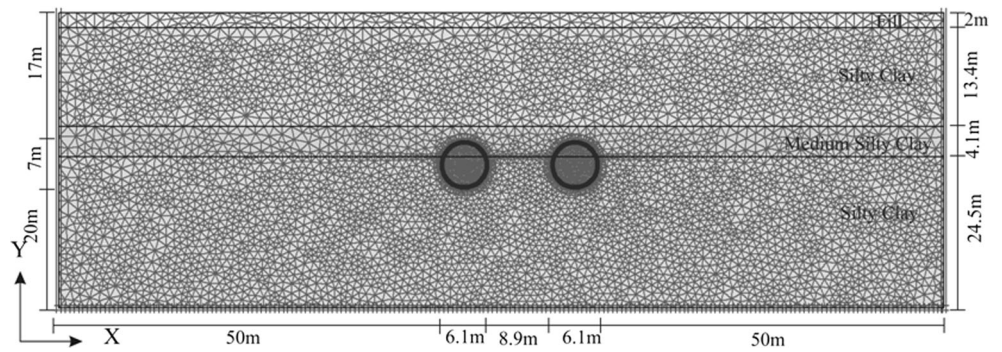**Fig. 4** Numerical discretization of the subsoil and the twin tunnels

Figure 5a and b show the ground settlements after the first and the second tunnels' construction, respectively, for the case of $V_L = 0.25\%$. The vibrations due to the TBM operations are not considered in these analyses. Note that in these figures, the ground heaving is shown as positive numbers, while the ground settlements are indicated by negative numbers. In both the figures, the ground settlement and the heaving are shown in millimeters.

The literature search on the settlements during tunneling indicates that very limited published data are available. The E-W metro tunnels are not yet constructed during the course of this study. So, in lieu of any field or published data, the numerical results in terms of ground settlements obtained from the present analyses are compared with the values obtained from the empirical relationships put forward by Mair et al. (1996) and FHWA (2009) to gain confidence.
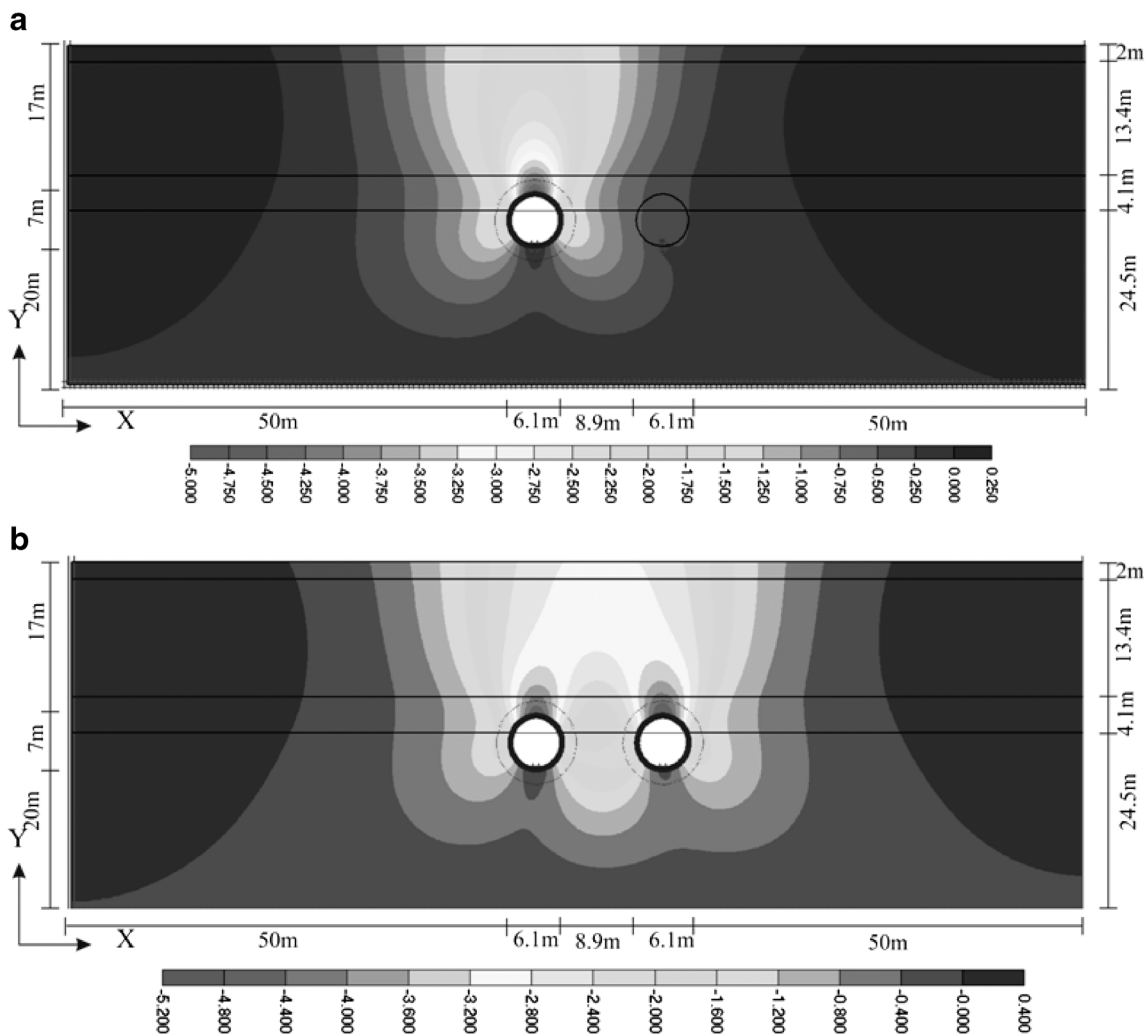
Fig. 5 Ground deformations (in mm). **a** After the construction of the first tunnel. **b** After the construction of both the tunnels

As per Mair et al. (1996), the settlement of the ground surface due to a tunneling is estimated as

$$S_V = S_{\max}e^{\frac{-y^2}{2i^2}} \tag{5}$$

where,

S_V vertical settlement
$S_{\max}$ maximum settlement above tunnel centerline
y horizontal distance from tunnel centerline
i distance to the point of inflection on the settlement trough = KZ_o
K trough width parameter = 0.5 for clay and = 0.25 for sands and gravels
Z_o depth of the tunnel spring line from the ground surface = 17.6 m in our case

$$S_{\max} = \frac{0.31V_LD^2}{KZ_o}$$

D diameter of the tunnel
V_L volume loss during tunnel construction

As per FHWA (2009), the settlement of the ground due to tunneling is estimated as

$$S_V = S_{\max}e^{\frac{-y^2}{2i^2}} \tag{6}$$

where,

S_V vertical settlement
$S_{\max}$ maximum settlement above tunnel centerline
y horizontal distance from tunnel centerline
i a parameter that may be obtained from a relationship between (Z/D) and (i/R)
Z depth of the tunnel crown from the ground surface = 17.6 m in our case
D diameter of the tunnel = 6.1 m in our case
R radius of the tunnel = $D/2$

In our case, Z/D = 2.9, and from the FHWA (2009), i/r = 2.5

Therefore, i = 7.625 m in our case

$$S_{\max} = \frac{V_L\pi r^2}{2.5i}$$

V_L volume loss during tunneling

Figure 6 shows the settlements of the ground surface after the first and the second tunnels are constructed at the

Brabourne Road by the numerical analyses and by the two empirical methods. In all the cases, the volume loss, V_L, during the tunneling is assumed to be 0.25%. Table 2 shows the maximum settlement and the settlements predicted at the centerlines of the tunnels and under the heritage structures.

It may be observed from the above figure and table that a maximum settlement of 3.83 mm is predicted by FHWA method at the centerline of the tunnel after the first tunnel is constructed. A maximum settlement of 2.83 mm is predicted by the numerical analyses and Mair et al. at the centerline of the first tunnel. The surface settlements at distances from the tunnels' centerline predicted by all the three methods differ significantly. The settlement trough is narrow for the FHWA method. It predicts almost zero settlement at the heritage building sites located between 34 and 45 m from the centerline of the first tunnel. The settlement trough predicted by the numerical method is the widest among the three. It predicts 0.3 mm and 0.11 mm at 34 m and 45 m from the centerline of the first tunnel.

After the construction of both the tunnels, a maximum settlement of 5.31 mm is predicted by the numerical analyses at the centerline between the tunnels. For this case also, the FHWA method shows a narrow settlement trough. It predicts 0.17 mm and 0.0017 mm of settlement at 19 m and 30 m from the second tunnel's centerline, which are the locations of Bethel Synagogue and Currency Building, respectively. As before, the settlement trough predicted by the numerical analyses is the widest. The numerical method predicts a settlement of 1.67 mm and 0.65 mm at 19 m and 30 m from the second tunnel. It may be noted that the settlement trough predicted by the numerical method is not symmetrical. It predicts more settlement towards the left side of the centerline located between the tunnels up to a horizontal distance of 35 m. Beyond a distance of 30 m, the settlements are not that significantly different. The surface settlements are 2 mm and 1.55 mm at 25 m away on the left side and the right side from the centerline between the two tunnels.

Figure 7 summarizes the settlements of the surface after the underground construction of the two tunnels at the Brabourne Road by the numerical method and the two empirical methods for the case of volume loss, V_L = 2% during the tunneling. Table 2 shows the maximum settlement and the settlements predicted at the centerlines of the tunnels and under the heritage buildings for this case.

In general, all the settlements have increased several times for the cases of V_L = 2% as compared with the cases with V_L = 0.25% (Table 3). After the first tunnel construction, a maximum settlement of 30.7 mm is predicted by FHWA method at the centerline of the tunnel. This value is ten times that for the V_L = 0.25%. The numerical analyses and Mair et al. predict 28.3 mm and 22.67 mm settlements at the centerline of the first tunnel. As before, the settlement trough is narrow for the FHWA method. It predicts almost no settlement at the heritage

Table 2 Ground settlement at different locations after the construction of the first and second tunnels with volume loss, $V_L = 0.25\%$

Method	Settlement (in mm)					
	Between centerline of 1st and 2nd tunnels (65 m)	At the centerline of 1st tunnel (55 m)	At the centerline of 2nd tunnel (70 m)	At Beth El Synagogue (89 m)	At Megen David Synagogue (90 m)	At Currency Building (100 m)
After the construction of 1st tunnel						
Numerical analyses	2.83			0.30	0.27	0.11
Mair et al.	2.83			0.01	0.007	0.00016
FHWA	3.83			0.0002	0.0001	0.0
After the construction of 2nd tunnel						
Numerical analyses	5.31	4.33	5.1	1.67	1.55	0.65
Mair el al.	4.3	3.8	3.8	0.51	0.42	0.37
FHWA	4.7	4.39	4.39	0.17	0.12	0.0017

building sites. As before, the settlement trough predicted by the numerical method is the widest among the three. It predicts 0.92 mm and 0.04 mm at 34 m and 45 m from the first tunnel.
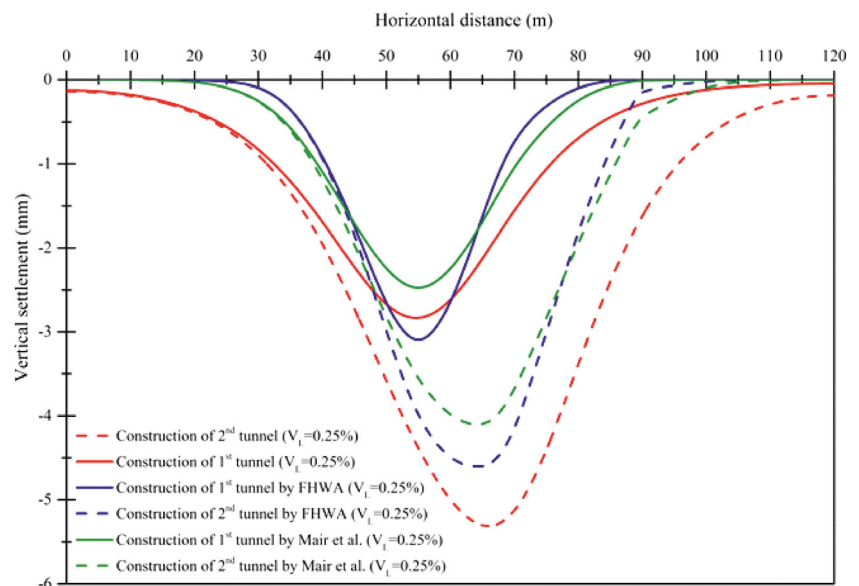
After the construction of both the tunnels, a maximum settlement of 43.5 mm is predicted by the numerical analyses at the centerline between the two tunnels. For this case also, the FHWA method shows a narrow settlement trough. It predicts 1.38 mm and 0.013 mm of settlement at 19 m and 30 m from the second tunnel, which are the locations of Bethel Synagogue and Currency Building, respectively. As before, the settlement trough predicted by the numerical analyses is the widest. The numerical method predicts a settlement of 8.14 mm and 1.76 mm at 19 m and 30 m from the second tunnel. As before, the settlement trough predicted by the numerical method is not symmetrical. It predicts more settlement towards the left side of the centerline located between the two

tunnels up to a horizontal distance of 35 m on both sides. The surface settlements are 4.4 mm and 4.0 mm at 35 m away on the left side and the right side from the centerline between the two tunnels.

Comparison with the field instrumentation data

During the course of the numerical analyses of the tunnels, no field instrumentation data was available. As a part of the study, all the three heritage buildings have been instrumented to monitor their settlements during the tunnel construction. Unfortunately, no monitoring instruments are placed over the centerline of the tunnels or within 15 m from the tunnels due to the presence of a very busy road (Brabourne Road) on

Fig. 6 Ground settlements after the construction of 1st and 2nd tunnels with $V_L = 0.25\%$

Fig. 7 Ground settlements after the construction of 1st and 2nd tunnels with V_L = 2%
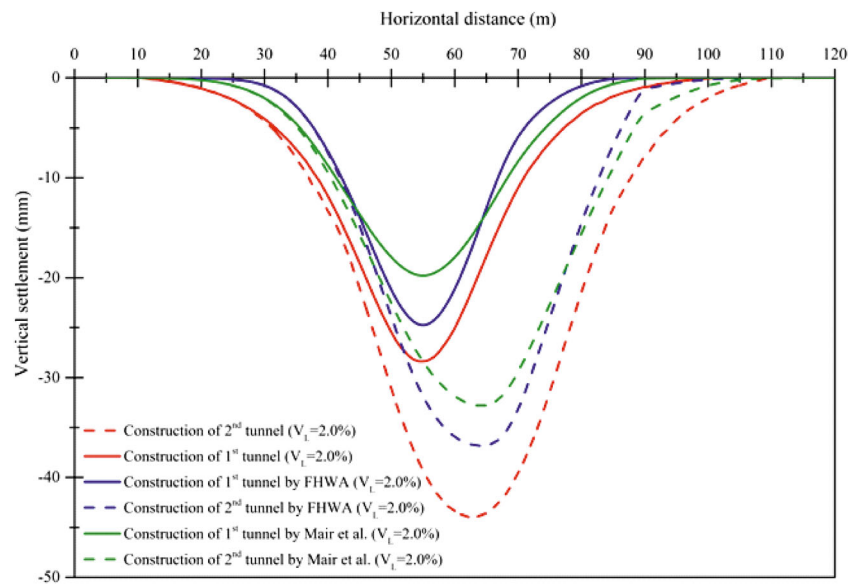
the top. The monitoring instruments installed in all the three heritage buildings are settlement markers, optical targets, tilt-meters, inclinometers, crackmeters, etc. The instruments are placed at different corners and at the middle of the buildings. Based on the settlement data for the extreme corners of the buildings, the maximum angular distortions within a building due to the tunnel construction are calculated. Table 4 shows the total settlements and the angular distortions estimated at the heritage structures after the construction of both the tunnels.

As may be seen from Table 4, for the Maghen David Synagogue and Bethel Synagogue, which are located 20 m and 19 m from the centerline of the 2nd tunnel, the numerical predictions are quite close to the measured settlements at these buildings. However, for the Currency Building which is locat-ed 30 m away, the recorded settlement is 3.9 mm, while the

numerical prediction has been 1.76 mm. The maximum angu-lar distortions predicted by the numerical method for the buildings located 19 to 20 m away are also found to be on the conservative side. While for the building located 30 m away, the maximum angular distortion is 1 in 1752 from the instrumentation readings as compared with 1 in 6087 from the numerical prediction. The angular distortions of the structures obtained by the analyses and from instrumentation readings are found to be very much within the admissible limit of 1/750. The settlements of these buildings are found to be very small by FHWA method, which has a very narrow settlement trough. The Mair et al. method has predicted settlements rea-sonably well for the buildings between 19 and 20 m but pre-dicts very less settlement for the building located 30 m away. One may note that near the centerline of the tunnels, both the empirical methods predict similar settlements as those

Table 3 Ground settlement at different locations after the construction of the first and second tunnels with volume loss, V_L = 2%

Method	Settlement (in mm)					
	Between centerline of 1st and 2nd tunnels (65 m)	At the centerline of 1st tunnel (55 m)	At the centerline of 2nd tunnel (70 m)	At Beth El Synagogue (89 m)	At Magen David Synagogue (90 m)	At Currency Building (100 m)
After the construction of 1st tunnel						
Numerical analyses		28.3		0.92	0.85	0.04
Mair et al.		22.67		0.085	0.061	0.0013
FHWA		30.7		0.0015	0.0008	0.0
After the construction of 2nd tunnel						
Numerical analyses	43.5	40.0	39.0	8.14	7.6	1.76
Mair el al.	34.1	30.3	30.3	4.05	3.35	0.30
FHWA	37.7	35.1	35.1	1.38	0.98	0.013

Table 4 Estimated total settlement and angular distortion due to tunnel construction

Heritage structure	Distance from centerline of 2nd tunnel (m)	Assumed volume loss (V_L)	Estimated maximum vertical settlement (mm)	Estimated maximum angular distortion	Field instrumentation data	
					Maximum settlement (mm)	Maximum angular distortion
Currency Building	30	0.25	0.65	1/50,000	3.9	1/1752
		2.0	1.76	1/6087		
Maghen David Synagogue	20	0.25	1.55	1/10,000	5.56	1/6501
		2.0	7.6	1/1650		
Bethel Synagogue	19	0.25	1.67	1/10,000	5.64	1/4821
		2.0	8.14	1/1600		

predicted by the numerical analyses. Looking at the field data, one may say that the settlement trough is quite wide in reality compared with that predicted in the numerical analyses and the empirical methods.

Since the settlement troughs are not symmetrical, it makes a significant difference if a structure is located on the left side of the 1st tunnel or on the right side of the 2nd tunnel. As the exact construction sequence of tunneling at Brabourne Road is not known at the time of this numerical study, the buildings under consideration are assumed conservatively to be on the left side of the first tunnel to be constructed. As already stated, the effects of the building stiffness and weights are not accounted for in the present numerical analyses. Detailed structural analyses are performed for the heritage buildings with the deformations obtained from this study to evaluate their conditions. These structural analyses are not part of this paper.

Effects of vibrations due to TBM operation

In the static analyses, the vibration of the ground due to the operation of the tunnel boring machines (TBM) and its effect on the nearby heritage buildings are not considered. The general feelings have been that the subsoil being silty clay or clayey silt, the vibration, and the settlement due to the vibration are not of any concern. Still, a dynamic analysis has been performed using the ABAQUS (1990) software to estimate the settlements induced by the ground vibrations during the excavation of the metro tunnels by TBM. In this study, the geometry of the problem considered in the numerical analyses remains same, as before. The heritage structures on the ground are not modeled. Instead, the ground vibration and the settlements at the locations of the designated structures are obtained for further consideration, if necessary.

For the nonlinear, time domain analysis in the ABAQUS program, the following dynamic equation of equilibrium is solved in discrete time increments:

$$[M]\{\ddot{u}(t)\} + [C]\{\dot{u}(t)\} + [K]\{u(t)\} = -[M][I]\{\ddot{u}_g(t)\} \quad (7)$$

where $[M]$ is the lumped mass matrix, $[K]$ is the stiffness matrix, $[I]$ is the influence matrix (equal to 1 in the direction of the application of motion, and 0 in the direction, where no motion is applied), and $[C]$ is the damping matrix of the soil (Rayleigh damping is used (Rayleigh and Lindsay (1945)). For performing the dynamic analysis in ABAQUS, the subsoil is discretized using 4-node plane strain element which takes into account the volumetric locking for incompressibility (Hughes 1987; Nguyen et al. 2007).

In the dynamic/vibration analyses, the boundary conditions are kept same as in the static analyses. The two side boundaries are on roller (horizontal movements restricted). The bottom boundary is also on roller with the vertical movement restricted. In addition to these, absorbing boundary elements are considered at all the three sides (two side boundaries and bottom) to minimize reflection and/or refraction of waves from them. As before, the two tunnels are not excavated at the same time at a given location. The tunnel linings are assumed to be elastic and impervious, as before, with the deformation modulus and the Poisson's ratio given by $E_{conc} = 3.162E+07$ kPa and $v_{conc} = 0.15$, respectively. In these analyses, the volume loss at the tunnels is not considered. In the dynamic analyses, the constitutive behaviors of the subsoil are modeled by two nonlinear material curves—one curve showing the degradation of the shear modulus (G/G_{max}) with shear strain and another curve showing increase in the damping ratio (β/β_{crit}) with the shear strain. Here, G is the shear modulus of the soil, G_{max} is the maximum shear modulus of the soil (obtained from static tests on the soil), β is the material damping of the soil, and β_{crit} is the critical damping of the soil. These two material curves completely define the shear behaviors of a soil under dynamic loading and they are often referred to as backbone curves. The material curves for the Kolkata (Brabourne Road) subsoil are obtained from a number of cyclic triaxial tests performed on the subsoil. For each soil, cyclic triaxial tests are performed at different confining pressures

and at different stress ratios. Figure 8 shows the cyclic triaxial test results for the undisturbed soil samples taken from 6.5 m, 9.5 m, 14 m, and 17 m depths near Brabourne Road area. The modulus degradation curve for the Kolkata subsoil is shown by the solid curve.

The ABAQUS program does not allow to specify directly the backbone curve for a soil. So, instead, the backbone curve of Ramberg-Osgood model (R-O model) (Ueng and Chen 1992) with proper fitting parameters is used in the analysis. The equation of the backbone curve of R-O model is given by

$$\frac{\gamma_{oct}}{\gamma_{ref}} = \frac{\tau}{\tau_{ref}} \left(1 + \alpha \left| \frac{\tau}{\tau_{ref}} \right|^{r-1} \right) \tag{8}$$

where γ_{ref}, τ_{ref}, α, and r are the model parameters. The strain is defined in terms of octahedral shear strain (γ_{oct}), which in case of a soil subjected to a harmonic shear strain under pure shear condition, is given by

$$\gamma_{oct} = \frac{2}{3} \sqrt{6 \frac{\gamma^2}{4}} \tag{9}$$

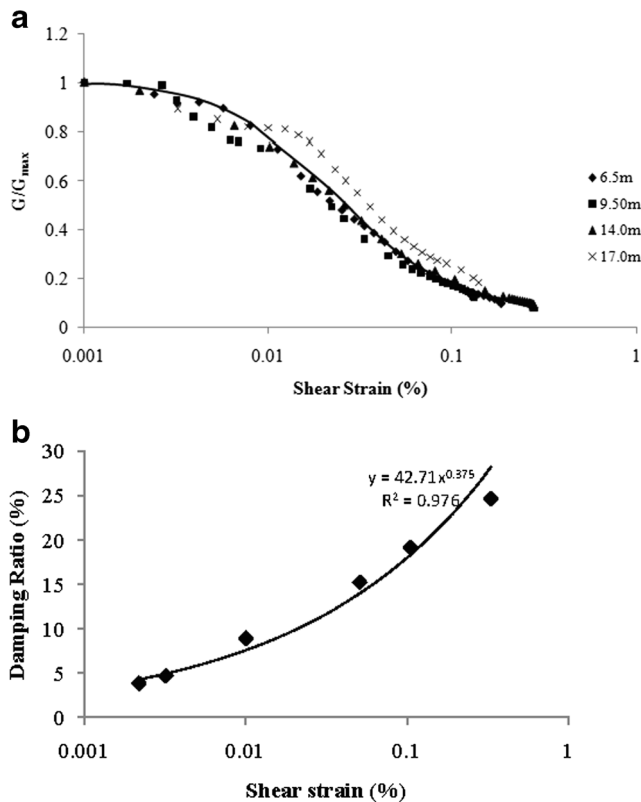where γ is the shear strain in the soil.

Fig. 8 Dynamic properties (shear modulus degradation and damping ratio) of Kolkata soils

The determination of the model parameters and the entire procedure for fitting the modulus reduction and damping ratio are elaborated in Ueng and Chen (1992). The comparison of the backbone curves for the Kolkata subsoil and that for the R-O model with parameters, $\gamma_{ref} = 0.021$, r (average of modulus reduction and damping ratio fit) = 2.5778 and α (average of modulus reduction and damping ratio fit) = 2.6595, is shown in Fig. 9a and b.

There is an existing metro line in Kolkata located at a depth of 16 m. No issue related to vibration has been reported. The present tunnels are located at 23 m depth, so vibration of buildings is not an issue. The analysis was done to check if any adverse settlement might result from this construction related vibrations. In the absence of any reliable data on the vibrations due to tunneling in Kolkata subsoil, an artificially generated white Gaussian noise is utilized to represent the vibrations due to tunneling as suggested by Mooney et al. (2014). Figure 10 shows the motions used in the dynamic analyses to represent the ground vibration during tunneling in the Kolkata subsoil.

This vibrational motion is applied in radial direction at the tunnel linings during the tunnel construction and its effect on the surrounding subsoil is analyzed. It may be noted that the vibrational motion is not applied at the same time to both the tunnels, since the tunnels are not constructed simultaneously at any given section. For this reason, a gap in the acceleration (refer to Fig. 11) is appearing. Figure 11 shows the response motions at the foundation of Currency Building (located 30 m away from the 2nd tunnel) due to the tunnel boring by TBM.

The maximum vibration of 0.002 m/s^2 is obtained at the Currency Building. This value is 0.003 m/s^2 at the other two buildings (Meghen David and Bethel Synagogues).

In engineering, the vibrations of the ground are typically expressed in terms of peak particle velocity (PPV). The PPV is defined as the vector sum of the maximum velocity components (V_{xmax}, V_{ymax}, V_{zmax}) of a motion, as shown in Eq. 10.

$$PPV = \sqrt{V_{xmax}^2 + V_{ymax}^2 + V_{zmax}^2} \tag{10}$$

The PPV is a measure of the damage due to vibrational motions. The damages to the structures or human discomfort are not directly caused by the velocities of the motions. Usually, it is the dynamic strains that result in the damages to the buildings and that is why they are of concern. The level of acceleration is usually linked to the human distress (Head and Jardine 1992). But, as PPV can be quantified easily and can be related to the observed effects of ground-borne vibrations, it is often utilized as an indicator of damage potential to the buildings and other structures. The maximum allowable limits for PPV due to tunneling and other constructions are suggested in a number of design codes (BS 7385-2 (1993), BS

Fig. 9 Comparison of the **a** modulus degradation (G/G_{max}) curve and **b** critical damping ratio (β/β_{crit}) curve for the Kolkata subsoil and those assigned in the dynamic analyses
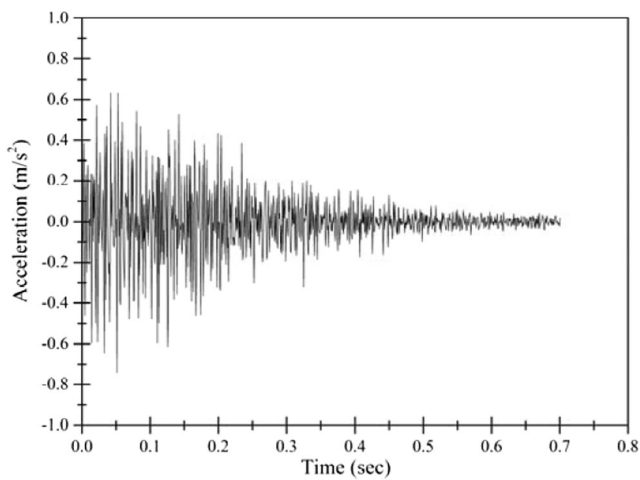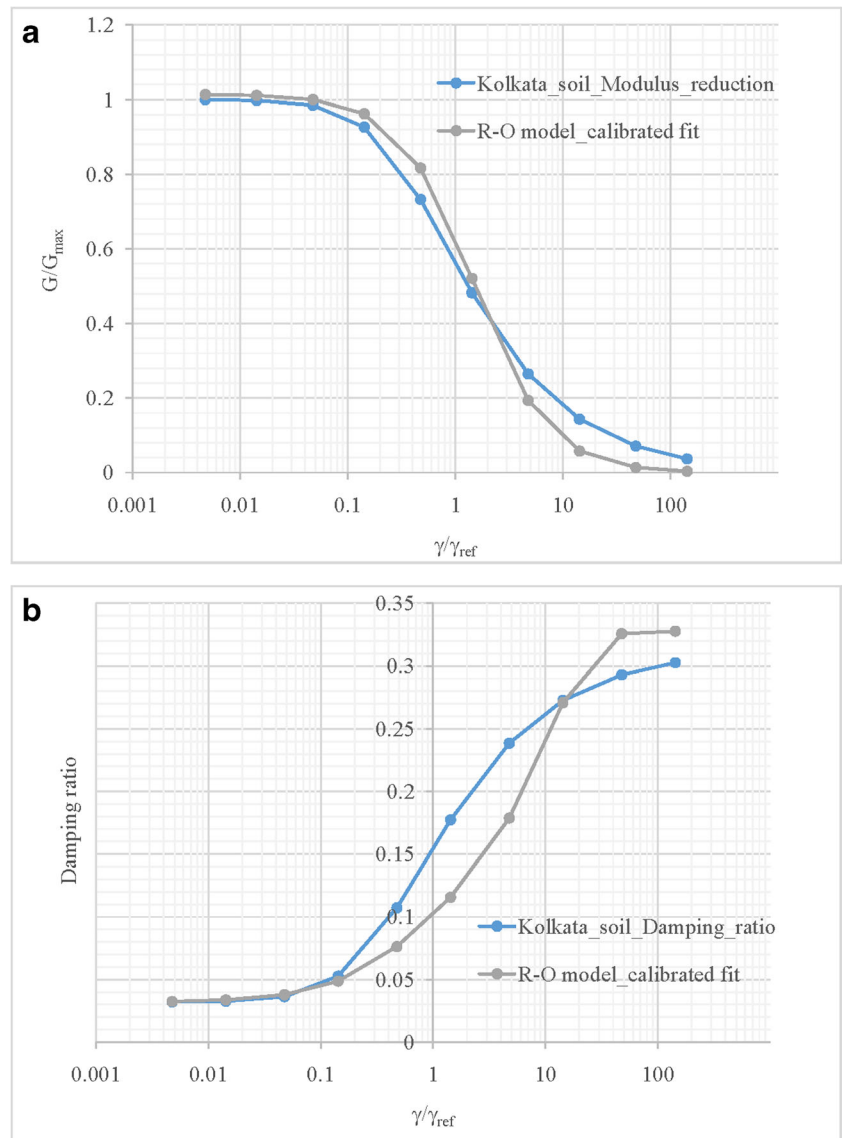
Fig. 10 Generated white Gaussian noise to model vibration due to TBM operation in a tunnel
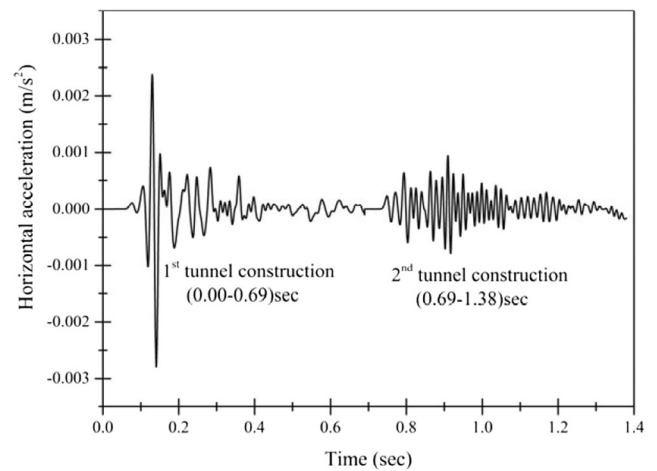
Fig. 11 Horizontal response at Currency Building due to tunnel construction

5228-4 (1992)). A maximum value for *PPV* of 1 mm/s is admissible by the metro rail authority of Kolkata for the underground tunnel construction. Figure 12 shows the calculated values of *PPV* with depth at 15 m, 20 m, and 25 m on both sides of the tunnels with both the tunnels constructed.

The maximum value of *PPV* is found to be 0.003 mm/s at the ground surface due to the tunnel construction. This value is far less than the allowable value of 1 mm/s.

The horizontal acceleration at Currency Building is only shown here. It does not imply that the vertical component of the motion has been ignored. As far as deformation is concerned, both the vertical and the horizontal components are considered. Figure 13 shows the vertical settlements at the Brabourne Road area due to the vibrations during the excavation of the two tunnels by TBM.

Figure 14 shows the settlements after the tunneling. The maximum vertical settlement at Currency Building due to the vibrations after the excavation of the twin tunnels is 0.009 mm from the dynamic analysis.

The dynamic analyses indicate that the maximum vertical settlement at Bethel Synagogue and Meghen David Synagogue is 0.01 mm due to the vibrations induced by the construction of the twin tunnels. All of these settlement values

Fig. 13 Vertical settlement at Currency Building due to TBM noise during construction of the first and second tunnel

are found to be very small for further consideration. The deformations and the accelerations on the building foundations are extremely small due to vibrations, and it is not significant, even if the duration of the vibrational motion due to the construction of the tunnels is increased several times. No field measurements for the ground and/or building vibration are
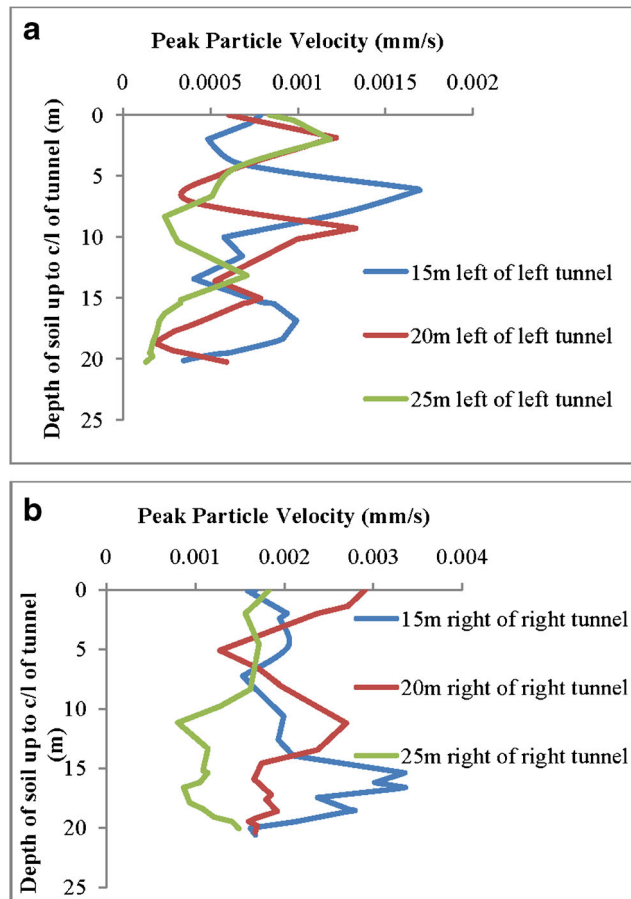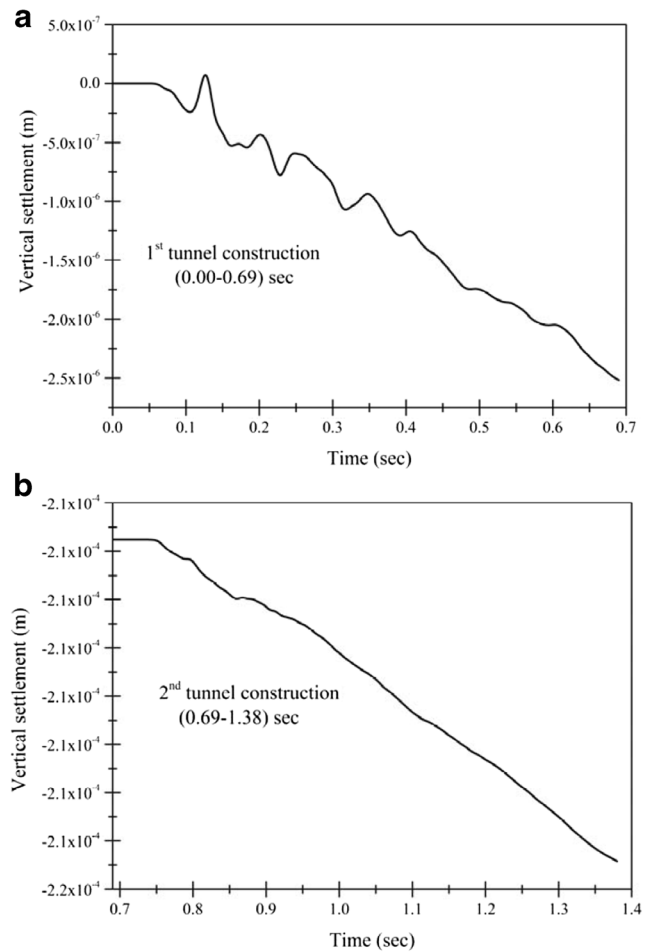

Fig. 12 Peak particle velocity (in mm/s) 15 m, 20 m, and 25 m away from the leftside and the rightside tunnels due to construction of both tunnels
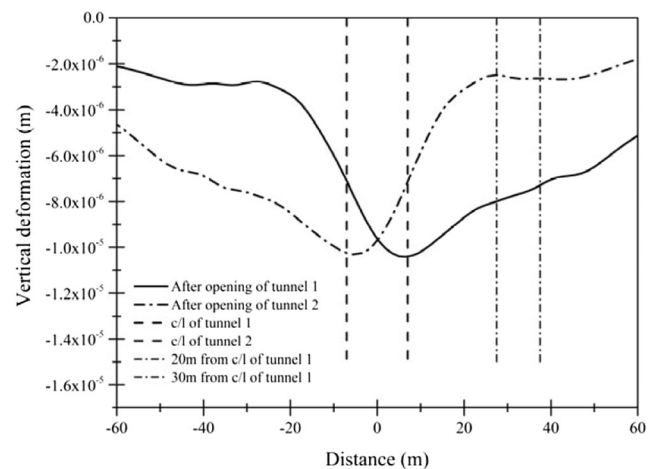

Fig. 14 Ground surface settlement profile after construction of tunnels

available. But no vibration related distress has been reported during the tunneling of the said portion, thus confirming the results of the vibration analyses at least qualitatively.

Conclusions

No adverse settlement has been observed or predicted for all the three heritage buildings due to the construction of the twin tunnels at 17.6 m depth from the ground. The vertical settlements of the ground surface predicted by the numerical analyses and the two empirical methods are found to be comparable at the tunnel centerlines. A maximum settlement of 43.5 mm (for $V_L = 2\%$) is predicted by the numerical analyses. The FHWA method predicts a maximum settlement of 37.7 mm, while the Mair et al. method predicts 34.1 mm (for $V_L = 2\%$). However, the values of the settlements predicted by these methods start to differ with distance from the tunnel centerlines. Around 19 to 20 m from the centerline of the 2nd tunnel, where the two synagogues are located, the numerical analyses predict a settlement of 7.6 to 8.14 m. The FHWA method predicts negligible settlement at this location. The Mair et al. predicts 3.35 to 4 mm settlements. The maximum settlements measured at these two buildings are between 5.56 and 5.64 mm. The maximum angular distortions measured at these buildings are between 1 in 4821 and 1 in 6501, well within the permissible limit of 1 in 750. The maximum angular distortions predicted by the numerical method are about 1 in 1600. Thus, the predictions made by the numerical analyses and Mair et al. are reasonably close to the measured settlement values up to a distance of 20 m from the centerline of the 2nd tunnel. However, beyond this, the predictions start to differ from the measured values of the settlement. At the Currency Building location, which is 30 m from the centerline of the 2nd tunnel, the measured settlement is 3.9 mm. The numerical prediction is 1.76 mm for maximum settlement. The Mair et al. predicts a maximum settlement of 0.3 mm at this location. Thus, one may say that the settlement trough is wider in the real case as compared with that in the numerical analyses or in the empirical methods. After 20 m from the 2nd tunnel centerline, the performances of the empirical methods are not reasonable. The numerical analyses also under-predict the settlements beyond 20 m. The two well established empirical methods considered in this study are developed based on the statistics of ground settlements in a limited number of tunneling cases and thus suffer from some limitations. On the other hand, a numerical method, like finite element analysis, is based on the nonlinear soil behaviors and realistic soil-structure interactions and thus expected to predict settlements due to subsurface tunneling more realistically. Thus, a finite element analysis is recommended for a similar study over the empirical methods. A Mohr-Coulomb material model has been utilized to model the subsurface soils in this study due to the availability to a limited amount of soil test data. One may guess that a better numerical soil model, which requires a lot more different test data on soils, might have yielded even better results at greater horizontal distances from the tunnels.

In the numerical analyses, the vibrations and the vertical settlements due to the tunneling are found to be very less. The peak particle velocity (PPV), obtained from the numerical analyses, at the ground surface is found to be about 0.003 mm/s. This value is significantly less than the allowable value of 1 mm/s. The actual vibrational motions generated during the tunnel excavation by TBM in Kolkata subsoil are not measured. These should be measured in the field for proper evaluation of the effect of tunneling related vibration on the adjacent structures on the ground. However, no vibration related distress has been reported during the tunneling of the said portion, thus confirming the results of the vibration analyses at least qualitatively.

References

ABAQUS (1990) User's manual, versions 4.8 and 3.4.3-1, Hibbitt, Karlssons & Sorensen, Inc., USA.

Bandyopadhyay S, Sengupta A, Reddy GR (2019) Development of correlation between SPT-N value and shear wave velocity and estimation of nonlinear seismic site effects for soft deposits in Kolkata city. Intl J of Geomech Geoeng:1–19. https://doi.org/10.1080/17486025.2019.1640898

BS 5228-4 (1992) Noise control on construction and open sites – part 4: code of practice for noise and vibration control applicable to piling operations.

BS 7385-2 (1993) Evaluation and measurement for vibration in buildings – part 2: guide to damage levels from ground borne vibration.

Camos C, Molin C, Arnau O (2014) Case study of damage on masonry buildings produced by tunneling induced settlements, International Journal of Architectural Heritage. Vol. 8(4):602–625. https://doi.org/10.1080/15583058.2012.704479

Festa D, Broere W, Bosch JW (2013) Tunneling in soft soil: on the correlations between the kinematics of a tunnel boring machine and the observed soil displacements, World Tunnel Congress 2013, Geneva, Underground – the Way to the Future!, G. Anagnostou & H. Ehrbar (eds), Taylor & Francis Group, London, pp. 2364-2371.

FHWA (2009) Technical manual for design and construction of road tunnels – civil elements, FHWA-NH1-10-034, U.S. Department of Transportation, Federal Highway Administration, Washington DC, Dec., pp 7–20

Gouw Tjie-Liong (2005) Tunneling induced ground movement and soil structure interactions. Seminar on Tunnel Technology in Civil Engineering, March 22. pp. 1-13.

Head JM, Jardine FM (1992) Ground-borne vibrations arising from piling. CIRIA Technical Note 142

Hughes TRJ (1987) The finite element method. Prentice-Hall International, Inc., New York

Kolkata Metro Rail Corporation (KMRC) (2015a) Application for permission for construction work of Mahakaran underground station

and tunnel near the protected monument of Currency Building along with assessment study report. June.

Kolkata Metro Rail Corporation (KMRC) (2015b) Application for permission for construction work of underground tunnel near the protected monument of Maghen David Synagogue along with assessment study report. June.

Kolkata Metro Rail Corporation (KMRC) (2015c) Application for permission for construction work of underground tunnel near the protected monument of Bethel Synagogue along with assessment study report. June.

Komiya K, Soga K, Akagi H, Hagiwara T, Bolton MD (1999) Finite element modeling of excavation and advancement processes of a shield tunneling machine, soils and foundations. Vol. 39(3):37–52

Kulhawy FH, Mayne PW (1990) Manual on estimating soil properties for foundation design. Ithaca, New York

Mair RJ, Taylor RN (1997) Bored tunneling in the urban environment. In: State-of-the-art report and theme lecture, Proceedings of 14th International Conference on Soil Mechanics and Foundation Engineering, Hamburg, Balkema, Vol. 4, pp 2353–2385

Mair RJ, Taylor RN and Burland JB (1996) Prediction of ground movements and assessment of risk of building damage due to bored tunneling. Geotechnical Aspects of Underground Construction in Soft Ground, Mair & Taylor (eds.), Balkema, Rotterdam, pp. 713-718, ISBN 90 5410 856 8.

Mooney M, Walter B Steele J and Cano D (2014) Influence of geological conditions on measured TBM vibration frequency. North American Tunneling Proceedings, G. Davidson et al. (eds.), SME, Colorado, USA, pp. 397-406.

Nagel F, Stascheit J, Meschke G (2010) Process-oriented numerical simulation of shield tunneling in soft soils, Geomechanics and Tunneling. Vol. 3(3):268–282

Nguyen TT, Liu GR, Dai KY, Lam KY (2007) Selective smoothed finite element method. Tsinghua Sci Technol 12:497–508

Peck RB (1969) Deep excavations and tunneling in soft ground, Proc. In: 7th International Conference Soil Mechanics and Foundation Engineering, Mexico City, State of the Art Volume, pp 225–290

Plaxisbv (2012) PLAXIS2D. Delft, Netherlands

Rayleigh JWS, Lindsay RB (1945) The theory of sound. Dover Publications, New York

Sugimoto M, Sramoon A (2002) Theoretical model of shield behavior during excavation. I: theory. J Geotech Geoenviron Eng 128(2): 138–155

Sugimoto M, Sramoon A, Konishi S, Sato Y (2007) Simulation of shield tunneling behavior along curved alignment in a multilayered ground. J Geotech Geoenviron Eng 133(6):684–694

Ueng T-S, Chen J-C (1992) Computational procedures for determining parameters in Ramberg-Osgood elasto-plastic model based on modulus and damping versus strain. DOI. https://doi.org/10.2172/6496483

USACE (1990). Settlement analysis. Engineering manual EM 1110-1-1904, Department of Army, U.S. Army Corps of Engineers, Washington DC20314-1000, USA.

Verruijt A (1997) A complex variable solution for a deforming circular tunnel in an elastic half plane. Int J Numer Anal Methods Geomech 21:77–89

Zhang D, Fang Q, Hou Y, Li P, Wong LNY (2013) Protection of buildings against damages as a result of adjacent large-span tunneling in shallowly buried soft ground. J Geotech Geoenviron Eng 139:903–913